Available online at www.sciencedirect.com
SCIENCE DIRECT®
Journal of Solid State Chemistry 177 (2004) 3536–3544
JOURNAL OF SOLID STATE CHEMISTRY
http://elsevier.com/locate/jssc

Eu^{3+} luminescence—a structural probe in $BiCa_4(PO_4)_3O$, an apatite related phosphate

N. Lakshminarasimhan and U.V. Varadaraju*

Materials Science Research Centre, Indian Institute of Technology, Madras, Chennai, Tamil Nadu, 600 036, India

Received 12 April 2004; received in revised form 5 June 2004; accepted 10 June 2004

Available online 11 August 2004

Abstract

Eu^{3+} luminescence is studied in apatite-related phosphate $BiCa_4(PO_4)_3O$. Compositions of the formula $Bi_{1-x}Eu_xCa_4(PO_4)_3O$ [$x = 0.05$, 0.1, 0.3, 0.5, 0.8 and 1.0] are synthesized and they are isostructural with parent $BiCa_4(PO_4)_3O$. Room temperature photoluminescence shows the various transitions $^5D_0 \rightarrow {}^7F_{J(=0,1,2)}$ of Eu^{3+}. The emission results of compositions with different Eu^{3+} content show the difference in site occupancy of Eu^{3+} in $Bi_{1-x}Eu_xCa_4(PO_4)_3O$. The intense $^5D_0$–$^7F_0$ line at 574 nm for higher Eu^{3+} content is attributed to the presence of strongly covalent Eu–O bond that is possible by substituting Bi^{3+} in the Ca(2) site. This shows the preferential occupancy of Bi^{3+} in Ca(2) site and this has been attributed to the $6s^2$ lone pair electrons of Bi^{3+}. This is further confirmed by comparing the emission results with $La_{0.95}Eu_{0.05}Ca_4(PO_4)_3O$.

Keywords: Apatite; Phosphate; Eu^{3+}; Luminescence; Structure probe; Bi^{3+}; Lone pair

1. Introduction

Eu^{3+} being the most important emitter in the red region of the visible spectrum, has been utilized extensively in color televisions and high efficiency fluorescent lamps [1]. Eu^{3+} has a simple electronic energy level scheme among the rare earth ions and the transitions are hypersensitive, i.e., they depend strongly on the chemical surroundings [2]. Because of these hypersensitive transitions, Eu^{3+} has been used as a local structure probe in determining the microscopic symmetries of different sites available in various host lattices, such as apatites [3–10] and eulytines [11]. Studies on the Eu^{3+} luminescence in $Sr_{10}(PO_4)_6F_2$ synthesized by coprecipitation method show that Eu^{3+} has OH^- or O^{2-} as neighboring ions and Eu^{3+} is present in a site with C_s symmetry that gives rise to the $^5D_0$–$^7F_0$ emission line at 576 nm [12]. Eu^{3+} luminescence has been studied in $Sr_{10}(PO_4)_6(OH)_2$ and an interesting result observed is the abnormal strong intensity of the forbidden $^5D_0$–$^7F_0$ transition and this is attributed to the covalent Eu^{3+}–O^{2-} bond that is formed between the Eu^{3+} in Sr(II) site and the free O^{2-} that is present close to this site to maintain the charge neutrality [13]. The splitting in the $^5D_0$–$^7F_0$ transition is attributed to the presence of Eu^{3+} in two sites labelled A_1 and A_2 corresponding to the 6*h* crystallographic position. This has been established by site selective laser spectroscopy wherein the Eu^{3+} in different sites could be excited selectively to study the emission behavior.

Eu^{3+} luminescence has been utilized as a structural probe in the calcium borohydroxyapatite wherein three lines for $^5D_0$–$^7F_0$ are observed for Eu^{3+} and they are assigned to three non-equivalent environments for Eu^{3+}; the *cis*- and *trans*-geometrical arrangements of the Eu^{3+} in the Ca(II) site with C_s symmetry and the Ca(I) site with C_3 symmetry [14]. It has been observed that the intensity of $^5D_0$–$^7F_0$ is two times stronger than $^5D_0$–$^7F_{1,2,3}$ emission. The abnormal behavior of the $^5D_0$–$^7F_0$ line is attributed to a covalent Eu–O bonding that arises in apatites. This type of behavior is also observed in Eu^{3+} doped Ba_2SiO_4 [15], $La_2Si_2O_7$ [16], mullite [16] and α-cordierite [17].

The interesting and useful properties evidenced in apatites depend on the occurrence of minor

*Corresponding author. Fax: +91-44-2257-0509.
E-mail address: varada@iitm.ac.in (U.V. Varadaraju).

0022-4596/$ - see front matter © 2004 Elsevier Inc. All rights reserved.
doi:10.1016/j.jssc.2004.06.021

substitutions that lead to minor alterations in the ideal apatite structure which has the space group of $P6_3/m$. For example, the substitution of Eu for Ca in calcium sulfoapatite, $Ca_{10-x}Eu_x(PO_4)_6S_{1+x/2}$ $[x = 0-1.3]$ changes the space group from $P6_3/m$ to $P6_3$ and it has been confirmed by Rietveld refinements [18]. This is due to the changes in the various Ca–O and P–O distances by the introduction of Eu^{3+} and S^{2-} and this results in the loss of mirror plane and two different environments for the Ca(1) site itself, namely Ca(1a) and Ca(1b). The recent review on the crystal chemistry of apatites also points out that there are minor deviations from the ideal $P6_3/m$ symmetry and the possible symmetries adopted by various apatite compounds are $P6_3$, $P\text{–}3$, $P\text{–}6$, $P2_1/m$ and $P2_1$ [19].

The compounds $BiCa_4(PO_4)_3O$ and $LaCa_4(PO_4)_3O$ have been reported recently [20]. They are isostructural with $BiCa_4(VO_4)_3O$ [21], which is closely related to the apatite structure except for the number of cationic sites available. $BiCa_4(VO_4)_3O$ crystallizes in hexagonal symmetry with the space group $P6_3$. In general, apatites with space group of $P6_3/m$ have only two types of cationic sites [6,22] whereas $BiCa_4(VO_4)_3O$ is reported to have three types of cationic sites viz., Ca(1), Ca(2) and Ca(3). The formula can be written as $Ca(1)_{0.9}Bi(1)_{0.1}Ca(2)_{2.1}Bi(2)_{0.9}Ca(3)(VO_4)_3O$. The Ca(1) and Ca(3) atoms occupy 2*b* and Ca(2) occupies 6*c* crystallographic sites. Both Ca(1) and Ca(2) atoms have 6-fold coordination and Ca(3) atom has 9-fold coordination with respect to oxygen. Ca(2) has an irregular hexa-coordinated polyhedron and the O(3) atom in the coordination sphere does not belong to any of the $-PO_4$ groups. Bi atom occupies both Ca(1) and Ca(2) sites with more occupancy in the low symmetry Ca(2) site.

In order to study the influence of chemical environment on the nature of emission of Eu^{3+} in different cationic sites and also to understand the preferential occupancy of Bi^{3+} among Ca(1) and Ca(2) sites in $BiCa_4(PO_4)_3O$, we have synthesized Eu^{3+} substituted phases and studied the luminescence properties. The luminescence of Eu^{3+} in $Bi_{0.95}Eu_{0.05}Ca_4(PO_4)_3O$ and $La_{0.95}Eu_{0.05}Ca_4(PO_4)_3O$ are compared to understand the preferential site occupancy of Bi^{3+}.

2. Experimental

2.1. Synthesis

Eu substituted compositions of the formula $Bi_{1-x}Eu_xCa_4(PO_4)_3O$ $[x = 0.05, 0.1, 0.3, 0.5, 0.8$ and $1.0]$ and $La_{0.95}Eu_{0.05}Ca_4(PO_4)_3O$ were synthesized by high temperature solid state reaction. The reactants were high purity Bi_2O_3 (Cerac, 99.9%), La_2O_3 (Indian Rare Earths, 99.9%), $CaCO_3$ (Cerac, 99.95%), Eu_2O_3 (Indian Rare Earths, 99.9%) and $NH_4H_2PO_4$ (Merck, 99%). La_2O_3 was preheated at 1100°C overnight. Stoichiometric quantities of the reactants were ground well and heated at 300°C for 6 h, 700°C for 12 h, 950°C for 24 h and finally at 1100°C for 24 h with intermittent grindings.

2.2. Characterization

The compounds were characterized by powder X-ray diffraction (XRD) (P3000, Rich Seifert) using Cu$K\alpha_1$ radiation at room temperature. Lattice parameters were calculated by least square fitting and KCl was used as internal standard. The diffraction patterns were indexed with the theoretically generated pattern using LAZY PULVERIX [23] program. IR spectra were recorded using KBr disc technique (IFS 66 V, Bruker). Photoluminescence excitation and emission spectra were recorded for the powder samples at room temperature using a spectrofluorometer (FP-6500, Jasco). An R-60 glass filter was used while recording the excitation spectra to remove the lower order reflections of the emission wavelength for which the excitation is recorded.

3. Results and discussion

3.1. Phase formation

Powder X-ray diffraction (XRD) patterns of select compositions $Bi_{1-x}Eu_xCa_4(PO_4)_3O$ $[x = 0.1,$ 0.3, 0.5, 0.8 and 1.0] are shown in Fig. 1. The XRD pattern of parent $BiCa_4(PO_4)_3O$ is given for comparison. It is evident from the XRD patterns that all the compositions have good crystallinity. We observe a small impurity line at 2-θ 31° for compositions $x = 0.3$ and 0.5 and this could be identified as β-$Ca_3(PO_4)_2$. All the lines can be indexed based on a hexagonal cell and the synthesized compositions are isostructural with parent $BiCa_4(PO_4)_3O$. The calculated hexagonal '*a*' and '*c*' lattice parameters are tabulated in Table 1. A decrease in the lattice parameters is observed with increasing Eu^{3+} content as shown in Fig. 2. This is due to the substitution of Bi^{3+} (1.02 Å) by smaller Eu^{3+} (0.95 Å) [24].

3.2. Infrared spectroscopy

Fig. 3a shows the IR spectrum of $BiCa_4(PO_4)_3O$ in the region 4000–400 cm^{-1} revealing there is no $-OH$ stretching vibrations (4000–3000 cm^{-1}) that confirms the composition is purely an oxyapatite. The IR spectra of all compositions are shown in Fig. 3b. The bands at around 1045, 550 and 600 cm^{-1} are assigned to $-PO_4$ stretching and bending vibrations [25]. The bands are

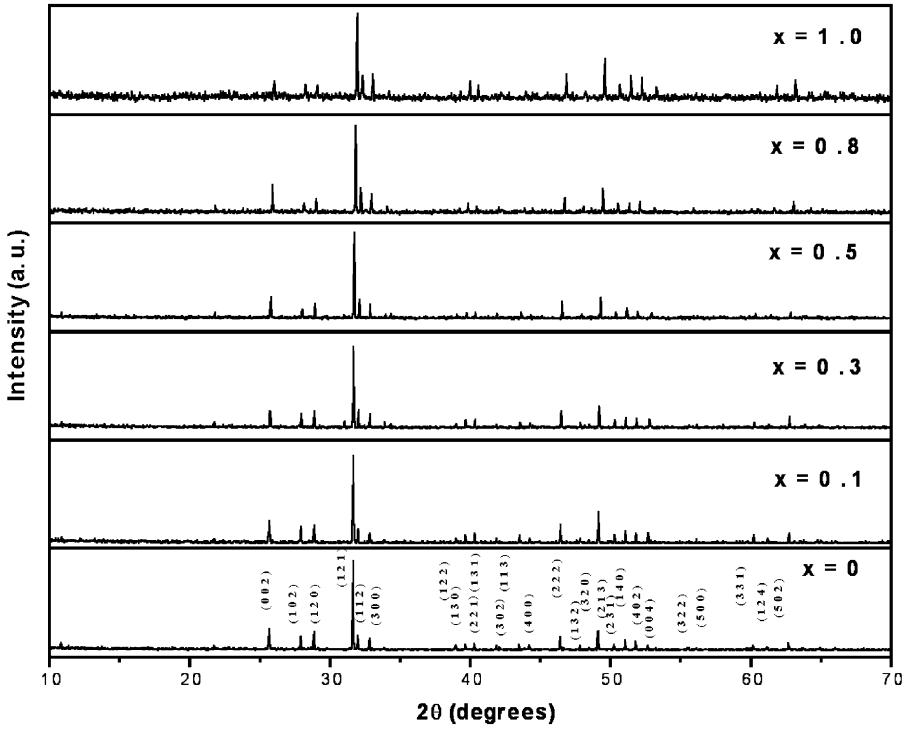

Fig. 1. Powder XRD patterns of $Bi_{1-x}Eu_xCa_4(PO_4)_3O$.

Table 1
Hexagonal a and c lattice parameters of $Bi_{1-x}Eu_xCa_4(PO_4)_3O$

x	a (Å)	c (Å)
0	9.469(4)	6.957(4)
0.1	9.464(4)	6.951(4)
0.3	9.456(4)	6.937(4)
0.5	9.443(4)	6.919(4)
0.8	9.429(4)	6.896(4)
1.0	9.409(4)	6.889(4)

broader for higher Bi^{3+} containing compositions and become narrower with increasing Eu^{3+} content. We have observed that these bands are narrow in the case of $La_{0.95}Eu_{0.05}Ca_4(PO_4)_3O$. This shows that Bi^{3+} plays an important role in making these bands broader when compared to $EuCa_4(PO_4)_3O$ and $La_{0.95}Eu_{0.05}Ca_4(PO_4)_3O$. In the crystal structure, the $-PO_4$ group shares all the four oxygens with the different Ca coordination spheres. There could be minor distortions in the $-PO_4$ group that shares its oxygens with Bi^{3+} due to the presence of $6s^2$ lone pair of electrons and this leads to the broadness of the bands. The shoulder observed at 630 cm^{-1} corresponds to the Bi–O bond stretching [20,25]. This shoulder becomes weaker in $Bi_{0.5}Eu_{0.5}Ca_4(PO_4)_3O$ and is completely absent in $EuCa_4(PO_4)_3O$ and $La_{0.95}Eu_{0.05}Ca_4(PO_4)_3O$ confirming the assignment to Bi–O stretching.

There is a weak absorption band observed at 526 cm^{-1} and this band becomes more distinct with increasing Eu^{3+} content. It has been reported for $Ca_{10-x}Eu_x(PO_4)_6O_{1+x/2}\square_{x/2}$ (□,vacancy), an absorption band observed at 545 cm^{-1} in both IR and Raman spectra is due to strong and covalent Eu–O bond, the oxygen of which does not belong to any of the $-PO_4$ groups [4]. Also in the case of $Sr_{10}(PO_4)_6(OH)_2$: Eu^{3+}, the Eu–O bond vibrations have been observed between 519 and 531 cm^{-1} in IR and Raman spectra and these are attributed to the presence of Eu^{3+} in two sites of 6*h* position [16]. In our results, the band at 526 cm^{-1} could be attributed to Eu–O (free) bond that is possible in Ca(2) site and its clear appearance for higher Eu^{3+} containing compositions shows the presence of Eu^{3+} in Ca(2) site only for higher Eu^{3+} containing phases.

3.3. Photoluminescence studies

3.3.1. $Bi_{1-x}Eu_xCa_4(PO_4)_3O$ [x=0.05, 0.1, 0.3, 0.5, 0.8 and 1.0]

The photoluminescence excitation and emission spectra of $Bi_{0.9}Eu_{0.1}Ca_4(PO_4)_3O$ is shown in Fig. 4. There are several excitations possible to the higher levels of Eu^{3+}. The broad band in the UV region (269 nm) corresponds to the Eu–O charge transfer (c.t.) band. The c.t. band is not the strong one and there exists a band at 320 nm overlapping with the c.t. band. This 320 nm band is absent in other compositions reported here. This band could be the Bi^{3+} excitation band. We have observed no Bi^{3+} emission in any of these compositions.

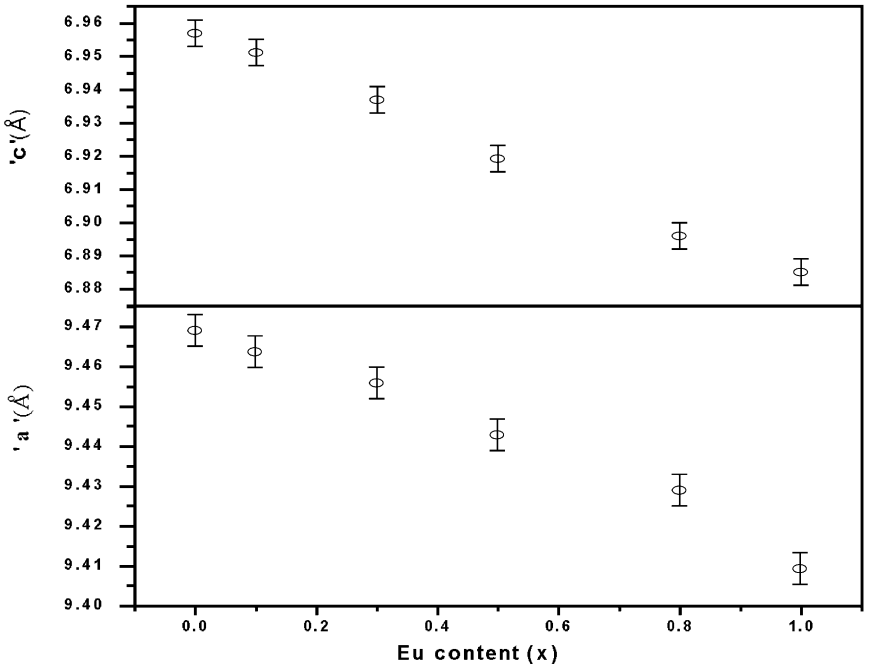

Fig. 2. Variation of '*a*' and '*c*' lattice parameters (Å) with Eu content in $Bi_{1-x}Eu_xCa_4(PO_4)_3O$.

The emission originates only from the $^5D_0$ level. The emission lines from higher levels such as $^5D_1$ are very weak. The phosphate lattice with high energy phonons (1045 cm^{-1}) couples well with higher levels and relaxes them to $^5D_0$ level which consequently becomes the excited level for all the emission transitions observed [26].

The emission spectra of all the compositions are shown in Fig. 5. The emission lines at 574–579 nm correspond to the $^5D_0 \rightarrow {}^7F_0$ transition of Eu^{3+}. The lines at 591 and 614–625 nm correspond to $^5D_0 \rightarrow {}^7F_1$ and $^5D_0 \rightarrow {}^7F_2$ transitions, respectively. It is well known that the transitions $^5D_0 \rightarrow {}^7F_0$ and $^5D_0 \rightarrow {}^7F_2$ are hypersensitive, i.e., they depend strongly on the chemical surroundings [2]. The $^5D_0 \rightarrow {}^7F_0$ transition is a forbidden one and will be present only when Eu^{3+} occupies sites with local symmetries of C_n, C_{nv} or C_s [27]. The number of lines for this non-degenerate $^5D_0 \rightarrow {}^7F_0$ transition is indicative of the number of Eu^{3+} ions in different crystallographic sites in the lattice. The $^5D_0 \rightarrow {}^7F_0$ transition has been observed in compounds with a strongly covalent Eu–O bond wherein the local symmetry of the Eu^{3+} changes to a pseudo $C_{\infty v}$ symmetry along the Eu–O bond and this favors $^5D_0 \rightarrow {}^7F_0$ transition to have higher intensity [4,28].

From the emission spectra of all compositions it is evident that the $^5D_0 \rightarrow {}^7F_0$ transition is present in all the cases and becomes more intense with higher Eu^{3+} concentration. A doublet for this transition is observed for phases with Eu^{3+} content 0.3 and higher. This shows that Eu^{3+} is present in two sites with different symmetries. The position of the additional line is at 574 nm and this line becomes more and more intense with increasing Eu content. This is possible only when there exist a strongly covalent Eu–O bond [4]. In other words, at low concentrations, Eu^{3+} substitutes Bi^{3+} in Ca(1) site and at higher concentrations, Eu^{3+} substitutes Bi^{3+} in both Ca(1) and Ca(2) sites. This is in good agreement with the crystal structure in which more of Bi^{3+} is in Ca(2) site than in Ca(1) site. Thus we can attribute the line at 577 nm to the Eu^{3+} in Ca(1) site and the line at 574 nm to Eu^{3+} in Ca(2) site. The relative intensity of the $^5D_0 \rightarrow {}^7F_0$ lines at 574 and 577 nm are different for different compositions. For phases with $x = 0.3$ and 0.5, the line at 577 nm is stronger than the one at 574 nm. For the phase with $x = 0.8$, the two lines have almost equal intensity and for the end member ($x = 1.0$), the 574 nm line is stronger than the 577 nm line. This shows that the distribution of Eu^{3+} in the two sites depends on the Eu^{3+} content in the lattice. Up to $x = 0.5$, Eu^{3+} occupies Ca(1) site more than the Ca(2) site and at $x = 0.8$, it is equally distributed in the two sites and in $EuCa_4(PO_4)_3O$, Eu^{3+} is present more in Ca(2) site than in Ca(1) site. This can be attributed to the highly covalent bond formed between Eu^{3+} and the free oxygen available. Our results are in good agreement with those of Piriou et al. [4] who reported similar behavior of increased intensity of the forbidden $^5D_0 \rightarrow {}^7F_0$ transition with increasing Eu^{3+} concentration in apatites of the formula $Ca_{10-x}Eu_x(PO_4)_6O_{1+x/2}\square_{x/2}$. The reason for this is the change of local symmetry for Eu^{3+}. As mentioned earlier, though the symmetry of the

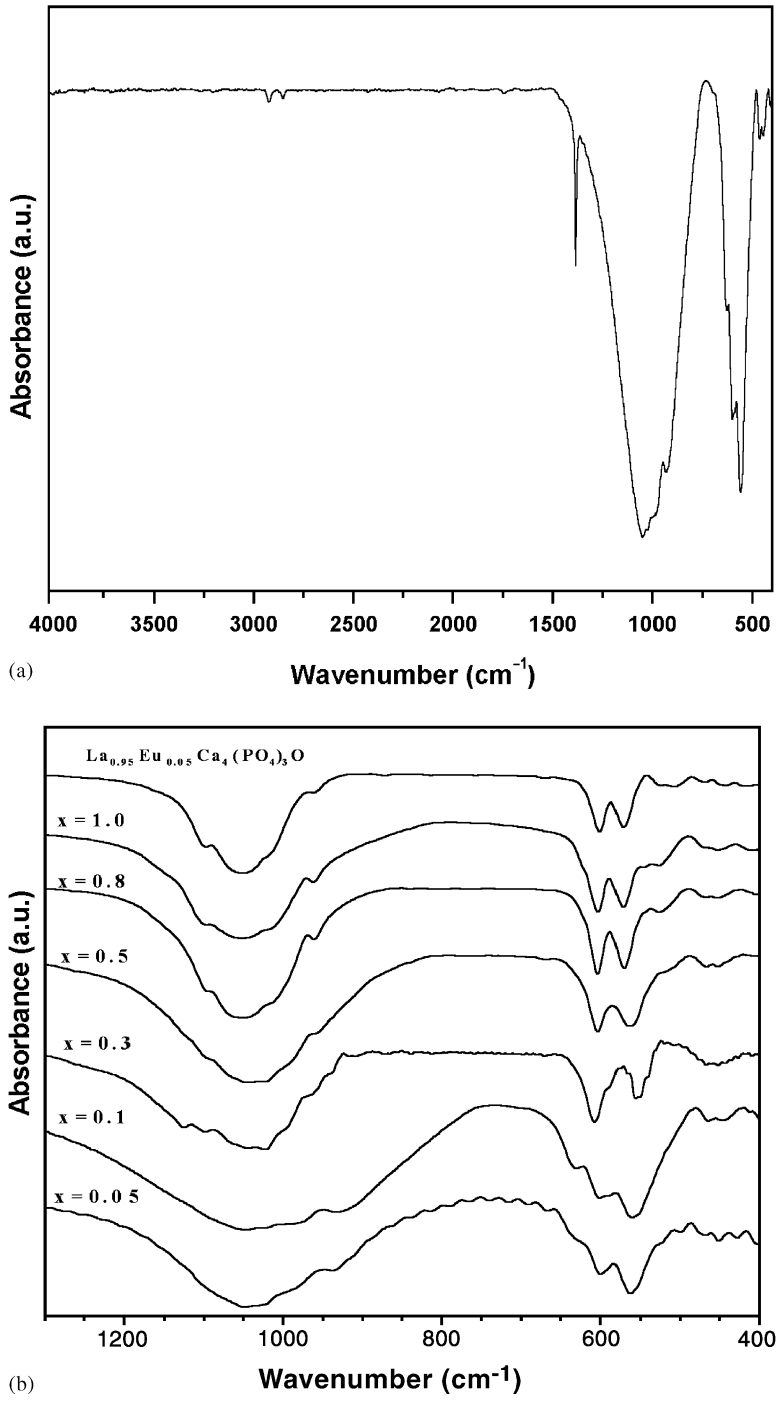

Fig. 3. (a) IR spectrum of $BiCa_4(PO_4)_3O$. (b) IR spectra of $Bi_{1-x}Eu_xCa_4(PO_4)_3O$ and $La_{0.95}Eu_{0.05}Ca_4(PO_4)_3O$.

Ca(2) site is C_s, the local symmetry changes to pseudo $C_{\infty v}$ symmetry because of the formation of a short and strongly covalent Eu–O (free) bond. Hence the local symmetry can be considered only along this bond. For $C_{\infty v}$ symmetry, the $^5D_0 \rightarrow {}^7F_0$ transition is allowed and the $^5D_0 \rightarrow {}^7F_2$ transition is forbidden. This results in the enhanced intensity of $^5D_0 \rightarrow {}^7F_0$ transition. In agreement with this, our results show that the preferential occupancy of Eu^{3+} in Ca(2) site makes the $^5D_0 \rightarrow {}^7F_0$ transition more intense for phases with higher Eu^{3+} content.

It is reported in oxysilicate apatites of the formula $Ca_2Ln_8(SiO_4)_6O_2$ [Ln = La, Gd and Y] that the smaller ions enter into the Ca(2) site where a free oxygen is available [5]. This Ca(2) site has more negative charge due to the coordinated free oxygen and hence a smaller and highly charged ion prefers this site and forms a strongly covalent bond with the free oxygen.

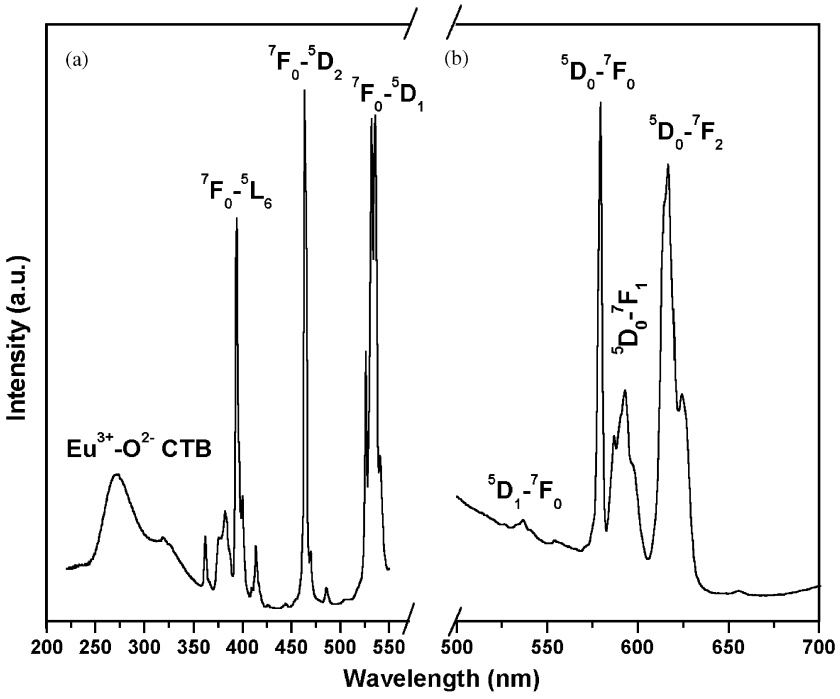

Fig. 4. (a–b) Excitatin and emission spectra of $Bi_{0.9}Eu_{0.1}Ca_4(PO_4)_3O$ [$\lambda_{exc.} = 395$ nm; $\lambda_{em.} = 617$ nm].

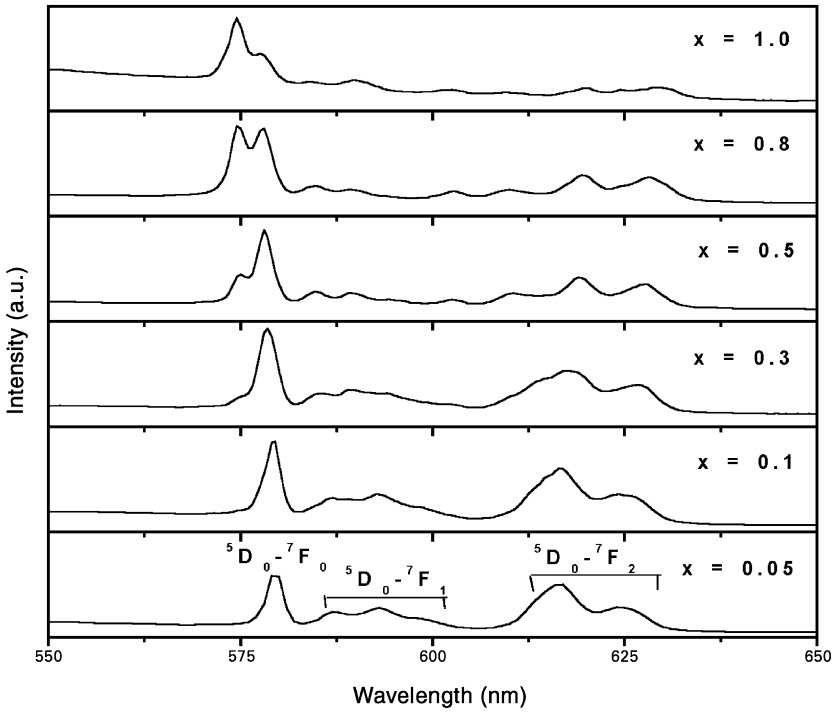

Fig. 5. Emission spectra of $Bi_{1-x}Eu_xCa_4(PO_4)_3O$ [$\lambda_{exc.} = 395$ nm].

This has been confirmed from the Eu^{3+} luminescence in the above-mentioned compounds. Based on this, one would expect Eu^{3+} occupying Ca(2) site even at low concentrations which is not observed in the present study. The reason for this behavior could be attributed to another important factor that controls the distribution of Eu^{3+} in the two sites and that is the site preference of Bi^{3+} ion with $6s^2$ lone pair electrons. In order to understand this further, we have studied Eu^{3+} luminescence in analogous $LaCa_4(PO_4)_3O$ wherein no such lone pair effects exist.

3.3.2. $Bi_{0.95}Eu_{0.05}Ca_4(PO_4)_3O$ and $La_{0.95}Eu_{0.05}Ca_4(PO_4)_3O$

The excitation and emission spectra of Eu^{3+} in these two lattices are shown in Figs. 6 and 7 respectively. In the excitation spectrum of $La_{0.95}Eu_{0.05}Ca_4(PO_4)_3O$, the Eu–O c.t. band has high intensity when compared to other excitation lines of Eu^{3+} and the emission lines of Eu^{3+} are weak in $La_{0.95}Eu_{0.05}Ca_4(PO_4)_3O$. In general,

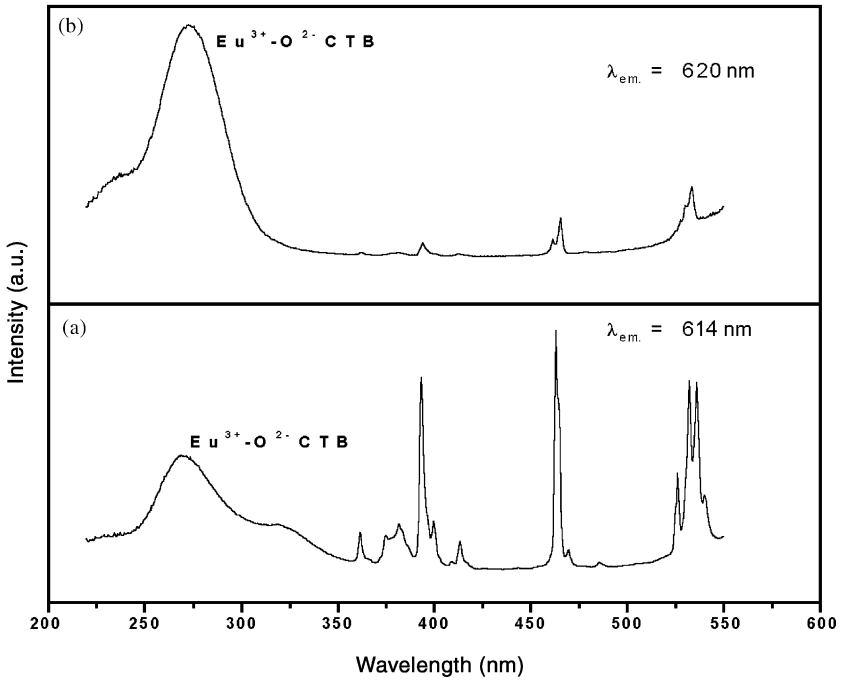

Fig. 6. Excitation spectra of (a) $Bi_{0.95}Eu_{0.05}Ca_4(PO_4)_3O$ [$\lambda_{em.} = 614$ nm] and (b) $La_{0.95}Eu_{0.05}Ca_4(PO_4)_3O$ [$\lambda_{em.} = 620$ nm].

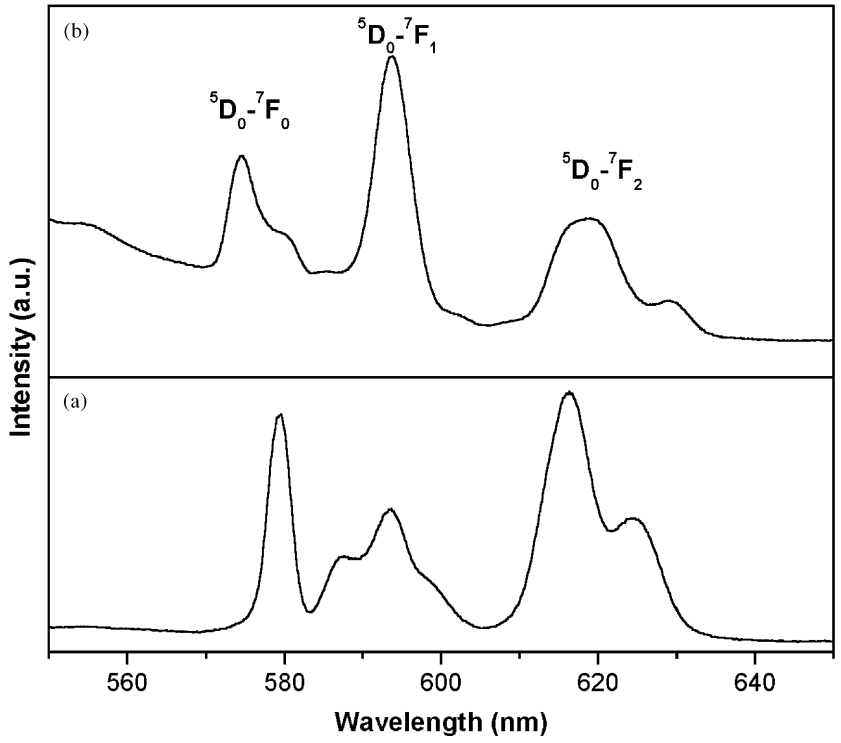

Fig. 7. Emission spectra of (a) $Bi_{0.95}Eu_{0.05}Ca_4(PO_4)_3O$ and (b) $La_{0.95}Eu_{0.05}Ca_4(PO_4)_3O$ [$\lambda_{exc.} = 395$ nm].

La containing compounds are not suitable hosts for Eu^{3+} to achieve high efficiency since La^{3+} makes the O^{2-} ion less polarized. This makes it easy to transfer an electron to Eu^{3+} ion resulting in the c.t. band to lie at low energy so that the non-radiative relaxation to the ground state becomes more probable [29].

The emission spectra of $La_{0.95}Eu_{0.05}Ca_4(PO_4)_3O$ show three major emissions of Eu^{3+} that could be assigned as $^5D_0$–$^7F_0$, $^5D_0$–$^7F_1$ and $^5D_0$–$^7F_2$ transitions. The features of $^5D_0$–$^7F_0$ transition are noteworthy. In $Bi_{0.95}Eu_{0.05}Ca_4(PO_4)_3O$, only one line is observed for $^5D_0$–$^7F_0$ transition at 579 nm. For $La_{0.95}Eu_{0.05}Ca_4(PO_4)_3O$ there is a band at 574 nm with a shoulder at 579 nm for $^5D_0$–$^7F_0$ transition. Also the position of this transition is different in both cases. In $La_{0.95}Eu_{0.05}Ca_4(PO_4)_3O$, it is at 574 nm indicating the presence of Eu^{3+} mainly in Ca(2) site that provides a short Eu–O bond. Thus in $La_{0.95}Eu_{0.05}Ca_4(PO_4)_3O$, Eu^{3+} occupies both Ca(1) and Ca(2) sites whereas in $Bi_{0.95}Eu_{0.05}Ca_4(PO_4)_3O$, Eu^{3+} occupies only Ca(1) site. This also suggests that such a low concentration of Eu^{3+} cannot substitute Bi^{3+} in Ca(2) site whose irregular hexa-coordinated geometry has enough space compared to Ca(1) site to accommodate the $6s^2$ lone pair electrons of Bi^{3+}. In $La_{0.95}Eu_{0.05}Ca_4(PO_4)_3O$, since La^{3+} has no such lone pair of electrons, Eu^{3+} substitutes La^{3+} in both Ca(1) and Ca(2) sites. Also the bond between Eu^{3+} and O^{2-}, the oxygen that does not belong to any of the $-PO_4$ groups, in Ca(2) site is shorter and more covalent. Thus, Eu^{3+} occupancy is more in Ca(2) site compared to that in Ca(1) site in $La_{0.95}Eu_{0.05}Ca_4(PO_4)_3O$ and this results in a stronger emission at 574 nm and a shoulder at 579 nm corresponding to Eu^{3+} in Ca(2) and Ca(1) sites, respectively. This preference of Eu^{3+} for Ca(2) site agrees well with the model explained by Blasse [5] based on the electrostatic potential.

Another interesting feature in $La_{0.95}Eu_{0.05}Ca_4(PO_4)_3O$, is the relative high intensity of magnetic dipole transition $^5D_0$–$^7F_1$. This magnetic dipole transition predominates when Eu^{3+} occupies a site in the lattice with a center of symmetry [1]. This shows that the Ca(1) and Ca(2) are more symmetric in $La_{0.95}Eu_{0.05}Ca_4(PO_4)_3O$ than in $Bi_{0.95}Eu_{0.05}Ca_4(PO_4)_3O$ because the $6s^2$ lone pair electrons of Bi^{3+} makes the environments less symmetric in the later compound especially in the Ca(2) site.

4. Conclusions

Eu^{3+} luminescence has been used as a structural probe in apatite related $BiCa_4(PO_4)_3O$. The $^5D_0 \rightarrow {}^7F_0$ transition of Eu^{3+} plays an important role in determining the occupancy of Eu^{3+} in different cationic sites. From the position of this line and relative intensity, it has been shown that at low concentrations of Eu^{3+}, the Bi^{3+} in Ca(1) site can only be substituted. At relatively high concentrations, Eu^{3+} is found to substitute Bi^{3+} in Ca(2) site. The reason for this is the $6s^2$ lone pair electrons of Bi^{3+} that makes Bi^{3+} prefer a site with irregular coordination geometry (Ca(2) site) in $BiCa_4(PO_4)_3O$. The comparative luminescence studies in $Bi_{0.95}Eu_{0.05}Ca_4(PO_4)_3O$ and $La_{0.95}Eu_{0.05}Ca_4(PO_4)_3O$ clearly show the presence of Eu^{3+} in one site in the former and two sites in the later compound. The results also show that the sites are more symmetric in the case of $La_{0.95}Eu_{0.05}Ca_4(PO_4)_3O$ and the $6s^2$ lone pair electrons of Bi^{3+} makes the Ca(2) site less symmetric in $Bi_{0.95}Eu_{0.05}Ca_4(PO_4)_3O$.

Acknowledgments

The author N. Lakshminarasimhan acknowledges the Council of Scientific and Industrial Research (CSIR), New Delhi for research fellowship.

References

[1] G. Blasse, B.C. Grabmaier, Luminescent Materials, Springer, Berlin, 1994.
[2] G. Blasse, A. Bril, W.C. Nieuwpoort, J. Phys. Chem. Solids. 27 (1966) 1587–1592.
[3] L. Boyer, B. Piriou, J. Carpena, J.L. Lacout, J. Alloys Compd. 311 (2000) 143–152.
[4] B. Piriou, D. Fahmi, J. Dexpert-Ghys, A. Taitai, J.L. Lacout, J. Lumin. 39 (1987) 97–103.
[5] G. Blasse, J. Solid State Chem. 14 (1975) 181–184.
[6] R. Jagannathan, M. Kottaisamy, J. Phys: Cond. Matter 7 (1995) 8453–8466.
[7] A. Zounani, D. Zambon, J.C. Cousseins, J. Alloys Compd. 207 (1994) 94–98.
[8] A.O. Wright, M.D. Seltzer, J.B. Gruber, B.H.T. Chai, J. Appl. Phys. 78 (1995) 2456–2467.
[9] R. Ternane, M.T. Ayedi, N.K. Ariguib, B. Piriou, J. Lumin. 81 (1999) 165–170.
[10] P. Martin, G. Carlot, A. Chevarier, C.D. Auwer, G. Panczer, J. Nucl. Mater. 275 (1999) 268–276.
[11] E.H. Arbib, B. Eloudi, J.P. Chaminade, J. Darriet, Mater. Res. Bull. 35 (2000) 761–773.
[12] A. Zounani, D. Zambon, J.C. Cousseins, J. Alloys Compd. 188 (1992) 82–86.
[13] R. El Ouenzerfi, N.K. Ariguib, M.T. Ayedi, B. Piriou, J. Lumin. 85 (1999) 71–77.
[14] R. Ternane, G. Panczer, M.Th. Cohen-Adad, C. Goutaudier, G. Boulon, N.K. Arigib, M.T. Ayedi, Opt. Mat. 16 (2001) 291–300.
[15] A.M. Pires, M.R. Davolos, O.L. Malta, J. Lumin. 72–74 (1997) 244–246.
[16] B. Piriou, M. Richard-Plouet, J. Parmentier, F. Ferey, S. Vilminot, J. Alloys Compd. 262–263 (1997) 450–453.
[17] B. Piriou, Y.F. Chen, S. Vilminot, Eur. J. Solid State Inorg. Chem. 35 (1998) 341–355.
[18] P.R. Suitch, A. Taitai, J.L. Lacout, R.A. Young, J. Solid State Chem. 63 (1986) 267–277.
[19] T.J. White, Dong. ZhiLi, Acta Crystallogr. B 59 (2003) 1–16.

[20] G. Buvaneswari, U.V. Varadaraju, J. Solid State Chem. 149 (2000) 133–136.
[21] J. Huang, A.W. Sleight, J. Solid State Chem. 104 (1993) 52–58.
[22] K. Sudarsanan, P.E. Mackie, R.A. Young, Mat. Res. Bull. 7 (1972) 1331–1338.
[23] K. Yvon, W. Jeitschko, E. Parthe, J. Appl. Cryst. 10 (1977) 73–74.
[24] R.D. Shannon, C.T. Prewitt, Acta Crystallogr. B 25 (1969) 925–945.
[25] R.A. Nyquist, R.O. Kagel, in Infrared Spectra of Inorganic Compounds, Academic Press, New York, 1971, p. 171.
[26] G. Blasse, A. Bril, J. Inorg. Nucl. Chem. 29 (1967) 2231–2241.
[27] G. Blasse, A. Bril, Philips Res. Repts. 21 (1966) 368–378.
[28] B. Piriou, A. Elfakir, M. Quarton, J. Lumin. 93 (2001) 17–26.
[29] G. Blasse, J. Chem. Phys. 45 (1966) 2356–2360.